JOURNAL OF EXPERIMENTAL AND THEORETICAL PHYSICS, 2024, Vol. 166, No. 3 (9), pp. 324–330

NUCLEI, PARTICLES, FIELDS, GRAVITY AND ASTROPHYSICS

MODELING OF HADRON CHARGE CORRELATIONS IN HEAVY ION COLLISIONS AT NICA ENERGIES

© 2024 E. E. Zabrodin, V. L. Korotkikh, I. P. Lokhtin*, S. V. Petrushanko, A. M. Snigirev, A. S. Chernyshov, G. Kh. Eyyubova

Lomonosov Moscow State University, Skobeltsyn Institute of Nuclear Physics,
119991, Lenisnkie Gory, Moscow, Russia

**e-mail: lokhtin@www-hep.sinp.msu.ru*

Received February 26, 2024
Revised May 13, 2024
Accepted May 14, 2024

Abstract. The model analysis of hadron charge correlations in heavy ion collisions was performed for energies available at NICA collider. The balance functions are considered as characteristics of such charge correlations. They represent the probability densities for oppositely charged particles to fall within a certain rapidity and azimuthal angle intervals. It has been shown that observed at STAR experiment at RHIC collider dependences of rapidity widths on centrality of gold-gold collisions at center-of-mass energies $\sqrt{SNN}$ =7.7 and 11.5 GeV per nucleon pair are reproduced by HYDJET++ model in the case of taking into account event-by-event conservation of electric charge for direct hadrons and finite values of isospin, strange and baryon chemical potentials.

Keywords: *relativistic heavy ion collisions, hadrons, charge correlations, Monte-Carlo event generators*

DOI: 10.31857/S004445102409e050

1. INTRODUCTION

The study of subnuclear matter properties under conditions of extremely high energy densities and temperatures achieved in relativistic heavy-ion collisions is one of the most dynamically developing areas of modern nuclear physics [1]. The first indications of the formation of a new state of strongly interacting matter — quark-gluon plasma (QGP) in heavy-ion collisions, such as anomalous suppression of J/ψ-mesons yield, thermal radiation of photons and lepton pairs, enhanced yield of "strange" hadrons, were obtained in fixed-target experiments at the SPS accelerator. The body of data obtained from experiments at RHIC and LHC colliders [2-8] (suppression of quarkonium and hard hadron yields, modification of hadron jet characteristics, strong azimuthal anisotropy of particle flow, long-range azimuthal correlations, etc.) indicates the manifestation of collective effects at the parton level and agrees with the assumption of the formation of hot matter with hydrodynamic properties ("quark-gluon liquid"). Further experimental and theoretical investigation of multiple particle production in relativistic nuclear collisions is related both to refining the parameters of hot QGP formed at high energies and to studying the dynamics of quark-hadron phase transitions, including the search for the "critical point" near their boundary through energy scan programs at RHIC and SPS, future CBM projects at the FAIR accelerator in GSI and MPD at the NICA collider at the JINR. Of significant interest is the study of various types of momentum, angular, and charge correlations of particles, carrying information about different stages of system evolution in nucleus-nucleus interaction.

The charge correlations of particles are characterized by "balance functions" (BF) – the probability density that oppositely charged particles are separated by certain intervals of rapidity and azimuthal angle [9–11]. Together with collective motion, the initial spatial separation of correlating charges leads to their further propagation in different

directions and the formation of spatial-momentum correlations between charge pairs. The widths of BFs are sensitive to the time during which charge separation occurs in the system, which opens up the possibility of using BFs to obtain information about the spatial-temporal characteristics of the particle emission region, including information about the presence and type of quark-hadron phase transition. Balance functions of charged particles have been studied in heavy-ion experiments at SPS [12], RHIC [13-15], and LHC [16-19]. One of the main experimental results obtained is that the width of BF for charged particles decreases when transitioning from peripheral to central nucleus-nucleus collisions, as well as with increasing energy of colliding beams. The width of BF is inversely proportional to the strength of collective flow in the system. Modern theoretical models poorly describe charge correlations of particles in heavy-ion collisions, particularly the dependence of BF widths on interaction centrality, which may indicate unaccounted mechanisms of such correlations in the models. Thus, an urgent task is to identify sources of charge correlations in various theoretical approaches and develop an adequate procedure for modeling such correlations that would allow describing experimental data over a wide energy range.

In this work, a model analysis of hadron charge correlations in heavy ion collisions is performed for the range of "intermediate" energies, which has already been partially studied at RHIC and will be studied in detail at NICA [20]. To simulate gold ion collisions at energies per nucleon pair in the center of mass system of $\sqrt{s_{NN}} = 7.7$ and 11.5 ГэВ the two- component Monte Carlo model HYDJET++ [21, 22], was used, where the final state of the nuclear reaction represents a superposition of soft hydrodynamic and hard jet components. In our previous work [23], we developed and implemented in the HYDJET++ model a procedure for accounting for charge correlations of direct hadrons in the soft component, which includes event-by-event conservation of electric charge at the “freeze-out” stage and allowed to reproduce the experimentally observed BF width dependence in lead ion collisions at LHC energies. In the present work, this procedure, originally developed for electrically neutral systems (corresponding to ultrarelativistic LHC energies), is generalized to the case of systems with electric charge imbalance, which corresponds, in particular, to the NICA energy range $\sqrt{s_{NN}}$ from 4 to 11 GeV.

2. CHARGE BALANCE FUNCTIONS OF OPPOSITELY CHARGED PARTICLES

The formalism of charge balance functions was proposed and developed in works [9, 10, 24-26]. The general definition of the charge balance function can be written as follows:

$$B_{ab}(\Delta y, \Delta\varphi) = \frac{1}{2}\int dW d(y_a - y_b - \Delta y)\, d(\varphi_a - \varphi_b - \Delta\varphi)\cdot \left[\frac{P_{a^+b^-} - P_{a^+b^+}}{P_{a^+}} + \frac{P_{a^-b^+} - P_{a^-b^-}}{P_{a^-}}\right], \quad (1)$$

where $dW = dy_a\, d\varphi_a\, dy_b\, d\varphi_b$, $\Delta y = y_a - y_b$ — relative rapidity of particles of types a and b, $\Delta\varphi = \varphi_a - \varphi_b$ — relative azimuthal angle of particles of types a and b, $P_{a^+b^-} = P_{a^+b^-}(y_a, \varphi_a; y_b, \varphi_b)$ — joint probability density to detect a positively charged particle of type a with rapidity y_a and azimuthal angle φ_a and a negatively charged particle of type b with rapidity y_b and azimuthal angle φ_b, $P_{a^+} = P_{a^+}(y_a, \varphi_a)$ — probability density to detect a positively charged particle of type a with rapidity y_a and azimuthal angle φ_a; other probability densities are introduced similarly. The projection of the charge balance function, for example, onto the Δy axis means the transformation

$$B(\Delta y) = \int B(\Delta y, \Delta\varphi)\, d\Delta\varphi$$

or corresponding summation in case of a histogram. The width of the BF projection is defined as $\langle\Delta y\rangle$, calculated as

$$\langle\Delta y\rangle = \frac{\int B(\Delta y)\Delta y\, d\Delta y}{\int B(\Delta y)\, d\Delta y} \approx \frac{\sum_i B_i \Delta y_i}{\sum_i B_i}. \quad (2)$$

For practical calculation of BF, the ultrarelativistic limit $y = \eta$ is taken and the following expression is used:

$$B_{ab}(\Delta\eta, \Delta\varphi) =$$

$$= \frac{1}{2}\left[\frac{1}{N_{a^+}}\frac{d^2N_{a^+b^-}}{d\Delta\eta d\Delta\varphi} + \frac{1}{N_{a^-}}\frac{d^2N_{a^-b^+}}{d\Delta\eta d\Delta\varphi} - \right.$$

$$\left. - \frac{1}{N_{a^+}}\frac{d^2N_{a^+b^+}}{d\Delta\eta d\Delta\varphi} - \frac{1}{N_{a^-}}\frac{d^2N_{a^-b^-}}{d\Delta\eta d\Delta\varphi}\right], \qquad (3)$$

where $N_{a^\pm}$ — number of positively charged particles of type a, $d^2N_{a^+b^-}/d\Delta\eta d\Delta\varphi$ — distribution of particle pairs a^+b^- by relative pseudorapidity and azimuthal angle; other distributions are introduced similarly. In general case, particles of types a and b may not belong to the same event. If particles belong to the same event — this corresponds to the "proper" charge balance function, if particles belong to different events — this corresponds to the "mixed" BF. To suppress the distortion introduced into the BF by the excess of positive charge characteristic for the low-energy part of RHIC energy range and planned NICA energy range, the distributions of the "mixed" BF are subtracted from the distributions of the "proper" balance function:

$$\frac{1}{N_{a^+}}\frac{d^2N_{a^+b^-}}{d\Delta\eta d\Delta\varphi} =$$

$$= \frac{1}{N_{a^+}}\frac{d^2N^S_{a^+b^-}}{d\Delta\eta d\Delta\varphi} - \frac{1}{N_{a^+}}\frac{d^2N^M_{a^+b^-}}{d\Delta\eta d\Delta\varphi}, \qquad (4)$$

where index "S" means that pairs are formed from particles selected from the same event ("proper" BF), index "M" — from two or more independent events ("mixed" BF).

In the experimental study of BF, additional distortion in its measurement is introduced by the finite angular acceptance of the detector. The BF correction for pseudorapidity acceptance is carried out according to [15

$$B(\Delta\eta \mid ¥) = \frac{B(\Delta\eta \mid \Delta\eta_{\max})}{(1 - \Delta\eta / \Delta\eta_{\max})}, \qquad (5)$$

where $B(\Delta\eta \mid ¥)$ is the balance function without restrictions on the pseudorapidity interval $B(\Delta\eta \mid \Delta\eta_{\max})$ is the BF calculated in a finite pseudorapidity interval, $\Delta\eta_{\max}$ is the maximum relative pseudorapidity of particle pairs available for measurement in the given experiment. In the present work, for correct comparison of simulation results with STAR data, the balance functions were constructed on the interva $0 < \Delta\eta < 2$ ($\Delta\eta_{\max} = 2$), and the widths of the corrected BF were calculated in the interval $0.1 < \Delta\eta < 1.6$.

3. HYDJET++ MODEL

For modeling multiple particle production in relativistic heavy ion collisions, this work uses the two-component Monte Carlo model HYDJET++, where the final state of nuclear reaction represents a superposition of soft hydrodynamic and hard jet components. Detailed description of HYDJET++ is provided in works [21, 22]. The basis for modeling the hard component of HYDJET++ is the PYQUEN (PYthia QUENched) event generator [27], which modifies the characteristics of parton jets obtained using the PYTHIA hadron-hadron interaction generator, taking into account multiple scattering and radiative and collisional energy losses of hard partons in QGP. Since at the energies under consideration, the dominant contribution to hadron multiplicity comes from the soft component, we will limit ourselves below to a brief presentation of the main characteristics of only the soft component of the model.

To describe the thermal (soft) hadron production in HYDJET++, a parameterization of relativistic hydrodynamics is used on the freeze-out hypersurface of the hadron matter cluster formed in nucleus-nucleus interaction, followed by resonance decay [30,31]. It is assumed that the chemical composition of the system is fixed at the stage of "chemical freeze-out" at a given temperature T^{ch} and chemical potentials μ_B, μ_I, μ_S, μ_C (for baryon charge, electric charge, strangeness, and charm, respectively). In this case, the hadron distribution in the rest frame of the fluid element has the form

$$f_i^{eq}(p^{*0}; T^{ch}, \mu_i, \gamma_s, \gamma_c) =$$

$$= \frac{g_i}{\gamma_s^{-n_i^s}\gamma_c^{-n_i^c}\exp([p^{*0} - \mu_i]/T^{ch}) \pm 1},$$

where p^{*0} is the hadron energy in the fluid element rest frame, g_i — spin factor, γ_s„ 1 and γ_c..1 — are strangeness suppression and charm enhancement coefficients respectively, n_i^s and n_i^n — number of

s-quarks anf c-quarks in hadron i, sign ± in the denominator accounts for the difference in quantum statistics for fermions and bosons. In this case, the number density of hadrons of type i (without considering coefficients γ_s and γ_c) can be written as

$$\rho_i^{eq}(T,\mu_i) =$$

$$= \frac{g_i}{2\pi^2} m_i^2 T \sum_{k=1}^{\infty} \frac{(\pm 1)^{k+1}}{k} \exp\left(\frac{k\mu_i}{T}\right) I_2\left(\frac{km_i}{T}\right)$$

where I_2 — is the modified Bessel function of the second kind, m_i is the particle mass. The model provides both the possibility of independent setting of input parameters at the chemical freeze-out stage (temperature, chemical potentials, coefficients γ_s and γ_c), and their calculation within phenomenological parameterizations [21].

BIn general, the stages of chemical freeze-out (when the ratio between the number of hadrons of different types stops changing) and thermal freeze-out (when the momentum distribution of hadrons stops changing) are separated in time and occur at different temperatures, T^{ch} and T^{th} respectively (with $T^{ch} \ldots T^{th}$). The multiplicity of hadrons in an event is modeled according to the Poisson distribution with mean for hadrons of each type , calculated on the freeze-out hypersurface in the effective thermal volume approximation: N_i for hadrons of each type i, calculated on the freeze-out hypersurface in the effective thermal volume approximation:

$$\overline{N_i} = \rho_i^{eq}(T) V_{eff}, \quad \rho_i^{eq}(T) = \int d^3 p^* f_i(p^{*0};T).$$

Here $\rho_i^{eq}(T)$ is the hadron density$i$ at temperature T, f_i and p^{*0} are respectively the distribution of hadron numbers and hadron energy in the rest frame of the fluid element, V_{eff} is the effective volume of the hadron emission region from the proper time hypersurface τ = const, calculated at the impact parameter of nucleus-nucleus collision b as

$$V_{eff} = \tau \int_0^{2\pi} d\varphi \int_0^{R(b,\varphi)} \sqrt{1 + \delta(b)\tanh^2 Y_T(r,b)\cos 2\varphi}\ \cdot$$

$$\cdot \cosh Y_T \tau(r,b) r\, dr \int_{\eta_{min}}^{\eta_{max}} Y_L(\eta) d\eta,$$

where $Y_L(\eta)$ and $Y_T(r,b)$ are the profiles of longitudinal (Gaussian function) and transverse (linear function) collective rapidities, $R(b,\varphi)$ is the transverse size of the hadron cluster in the azimuthal direction φ, $\delta(b)$ is the parameterization of the momentum azimuthal anisotropy of the source. The characteristics of stable particles and resonances are taken from the SHARE table [32].

The HYDJET++ model was initially developed for ultrarelativistic RHIC and LHC energies, but was later adapted for the intermediate energy range of NICA and FAIR. Based on the comparison of simulation results with STAR experiment data at RHIC on yields and momentum spectra of identified hadrons in gold ion collisions at energies $\sqrt{s_{NN}} = 7.7$ and 11.5 GeV [33], the main parameters of HYDJET++ were tuned [34], which allowed this model to be used for studying prospects for measuring certain physical effects in experiments at NICA. In particular, using the HYDJET++ model for heavy ion collisions at NICA energies, the influence of various “global observables” (multiplicity, collective flows) on multi-particle correlations determined by the factorial moments method was investigated [35, 36].

4. CHARGE CORRELATIONS OF DIRECT HADRONS IN HYDJET++

In the "standard" version of the HYDJET++ model, the sources of hadron charge correlations are resonance decay and parton jet fragmentation. In work [23], it was shown that these sources are insufficient to describe the experimentally observed dependence of the BF width in lead ion collisions at LHC energies, and a procedure was developed to account for charge correlations of direct hadrons, including event-by-event conservation of electric charge at the "freeze-out" stage, which allowed to reproduce experimental data. Direct hadrons refer to hadrons formed directly on the chemical freeze-out hypersurface, as opposed to particles resulting from resonance decay. This procedure involves random selection of half of the direct charged hadrons from the model's soft component (the remaining half is removed from the event), for each of which a "partner particle" is generated with the opposite electric charge sign and the same transverse momentum value. The pseudorapidity η_2 and azimuthal angleφ_2 of such partner particle are distributed around the

pseudorapidity η_1 and azimuthal angle φ_1 of the first particle according to the Gaussian distribution:

$$P_{\mu,\sigma}(x) = \frac{1}{\sqrt{2\pi\sigma^2}} \exp\left[\frac{(x-\mu)^2}{2\sigma^2}\right] \qquad (6)$$

where $\mu = \eta_1, \varphi_1$, $\sigma = \sigma_\eta, \sigma_\varphi$ and $x = \eta_2, \varphi_2$. The width values of these distributions σ_η and σ_φ characterize the strength of charge correlations of direct hadrons and are additional model parameters that are selected by comparing with experimental data on corresponding FB widths.

It is important to note that the procedure described above for accounting for charge correlations of direct hadrons is applicable to electrically neutral systems (i.e., with zero values of isospin, strange, and baryon chemical potentials), which corresponds to ultrarelativistic LHC energies. In the present work, this procedure has been generalized to the case of systems with an imbalance of positive and negative electric charges and finite values of chemical potentials, which corresponds to the NICA energy range. To account for the electrical imbalance of the system, the procedure for introducing charge correlations is carried out separately for each type of direct charged hadrons in the soft component of the HYDJET++ model. Among hadrons of the i th type, $N_i = (Q_i^+ + Q_i^-)/q_i$ positive for $N_i > 0$ or negative for $N_i < 0$ charged hadrons are randomly selected, which remain in the event without modifications (here Q_i^+ is the total charge of positively charged hadrons of i th type, Q_i^- — is the total charge of negatively charged hadrons, q_i is the absolute value of the electric charge of this hadron type). Preserving N_i direct hadrons unchanged ensures the preservation of charge imbalance. The previously described procedure for introducing charge correlations is applied to the remaining "electrically neutral" part of direct charged hadrons of the event.

Table 1: Ratios of multiplicities of oppositely charged hadrons in central collisions at RHIC energies and chemical potential values in HYDJET++

		p^+/p^-	K^+/K^-	$p/\bar{p}$
7.7 GeV	RHIC STAR	0.93±0.12	2.70±0.31	1.41±24
	HYDJET++	0.89	2.70	130
	$\mu_{I,S,B}$, *MeV*	6	100	429
11.5 GeV	RHIC STAR	0.95±0.14	2.03±0.28	29.3±5.3
	HYDJET++	0.93	1.99	28.2
	$\mu_{I,S,B}$, *MeV*	7	72	313

Table 2: Parameter values σ_η in the modified version of HYDJET++, model, selected to describe STAR data

Centrality, %	σ_η	
	$\sqrt{s_{NN}} = 7.7 GeV$	$\sqrt{s_{NN}} = 11.5 GeV$
−5	1.25	1.00
−10	1.35	1.08
−20	1.47	1.17
−30	1.62	1.30
−40	1.80	1.44
−50	2.00	1.60

5. SIMULATION RESULTS AND COMPARISON WITH RHIC DATA

Table 1 shows the ratios of multiplicities of positively and negatively charged hadrons of different types in the central rapidity region $|y| < 0.1$ for most central gold ion collisions at energies $\sqrt{s_{NN}} = 7.7$ and 11.5 GeV (HYDJET++ results and STAR data [33]). Table 1 also shows the values of isospin μ_I, strange μ_S and baryon μ_B chemical potentials in HYDJET++. The results for the modified and unmodified versions of HYDJET++ coincide and are close to the experimental data. We have also verified that the modification does not change the yields and momentum spectra of identified hadrons, maintaining the description of STAR data on these observables [34] achieved earlier in the unmodified version of the model.

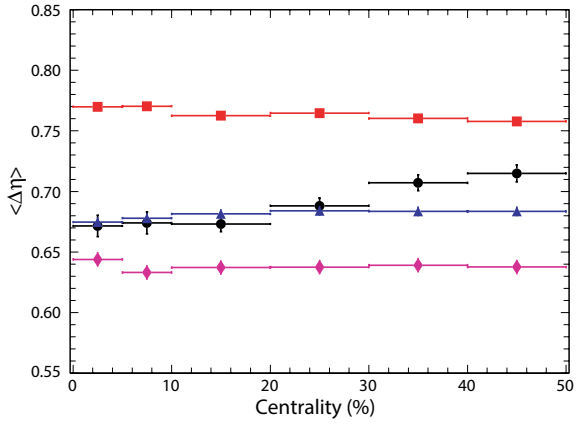

Fig. 1. Dependence of the balance function rapidity width on collision centrality Au+Au at energy $\sqrt{s_{NN}} = 7.7GeV$. Circles — STAR data [15], diamonds and triangles — simulation results with unmodified and modified versions of HYDJET++ respectively, squares — UrQMD simulation results UrQMD

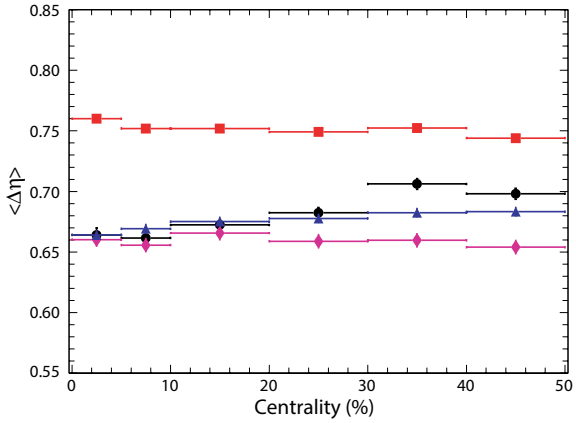

Fig. 2. Dependence of the balance function rapidity width on collision centrality Au+Au at energy $\sqrt{s_{NN}} = 11.5GeV$. Circles — STAR data [15], diamonds and triangles — simulation results with unmodified and modified versions of HYDJET++ respectively, squares — UrQMD simulation results UrQMD

Subsequently, to verify the effectiveness of the developed procedure for accounting for charge correlations of direct hadrons, event simulation and selection were conducted under the same conditions as in the STAR experiment [15]. Using unmodified and modified versions of the HYDJET++ event generator, gold ion collisions were simulated at energies $\sqrt{s_{NN}} = 7.7$ and 11.5 GeV for six centrality classes (range from 0 to 50%). For analysis, charged particles with transverse momenta $0.2 < p_T < 2$ GeV/c in the pseudorapidity range $|\eta| < 1$ were selected. We limited ourselves to the centrality range 50 %, which corresponds to maximum values of impact parameter $b \sim 1.5R_A$, where R_A is the nuclear radius, since the hydrodynamic description used may not be well applicable for very peripheral collisions in the considered energy range.

Figure 1 and 2 show the dependence of the rapidity widths of the BF on the centrality of gold ion collisions at energies of $\sqrt{s_{NN}} = 7.7$ and 11.5 GeV, respectively. Measurement uncertainties are only visible for the data, statistical uncertainties of model results are within marker size. Table 2 shows the used values of parameter for rapidity correlations of direct charged hadrons in the modified version of HYDJET++. In addition to HYDJET++ results, the figures also show results from the microscopic transport model UrQMD [37], based on hadron cascading and widely used for modeling heavy ion collisions at intermediate energies. It can be seen that the unmodified version of HYDJET++ and UrQMD do not reproduce the STAR-measured dependencies of BF rapidity widths on centrality, underestimating (HYDJET++, except for 20% the most central collisions at the most central collisions at $\sqrt{s_{NN}} = 11.5$) or overestimating (UrQMD) the experimental values. The introduction of charge correlations of direct hadrons in the HYDJET++ model allows for significantly improved description of the data in the considered range of energies and centralities. The values of BF rapidity widths are reproduced with good accuracy up to 30% centrality. The slight underestimation of data observed for more peripheral collisions may indicate limited applicability of the used model (as well as statistical approximation in general) in the case of relatively small multiplicities.

6. CONCLUSION

Within the HYDJET++ model, charge correlations of hadrons in heavy ion collisions were studied for the intermediate energy range corresponding to the RHIC energy scan program and planned NICA collider energies. As characteristics of charge correlations, balance functions were considered, which represent probability densities that oppositely charged particles are separated by certain intervals of rapidity and azimuthal angle. Modern theoretical models poorly desribe charge correlations of particles in heavy ion collisions, particularly the dependence of BF widths on interaction centrality, which may indicate unaccounted mechanisms of such correlations in the models.

A generalization of the previously developed procedure for accounting charge correlations of direct hadrons for electrically neutral systems (corresponding to ultrarelativistic LHC energies) was carried out for systems with imbalance of positive and negative charges (corresponding to intermediate NICA and RHIC energies). It is shown that the experimentally observed dependencies of rapidity widths of the balance function on centrality of gold ion collisions at energies $\sqrt{s_{NN}} = 7.7$ and 11.5 GeV can be reproduced by the HYDJET++ model in case of introducing event-by-event conservation of electric charge of direct hadrons and accounting for finite values of isospin, strange and baryon chemical potentials. Thus, the proposed approach for modification of statistical hadron production allows describing charge correlations in heavy ion collisions in a wide energy range (from LHC to NICA).

ACKNOWLEDGMENTS

The authors thank L. V. Bravina and A. I. Demyanov for useful discussions.

FUNDING

This work was supported by the Russian Science Foundation (grant No. 24-2200011).

REFERENCES

1. J. W. Harris and B. Muller, arXiv:2308.05743.

2. I. Arsene, et al. (BRAHMS Collaboration), Nucl. Phys. A 757, 1 (2005).

3. B. B. Back, et al. (PHOBOS Collaboration), Nucl. Phys. A 757, 28 (2005).

4. J. Adams, et al. (STAR Collaboration), Nucl. Phys. A 757, 102 (2005).

5. K. Adcox, et al. (PHENIX Collaboration), Nucl. Phys. A 757, 184 (2005).

6. B. Muller, J. Schukraft, and B. Wyslouch, Ann. Rev. Nucl. Part. Sci. 62, 361 (2012).

7. N. Armesto and E. Scomparin, Eur. Phys. J. Plus 131, 52 (2016).

8. ALICE Collaboration, arXiv:2211.04834.

9. D. Drijard et al., Nucl. Phys. B 155, 269 (1979).

10. S. Bass, P. Danielewicz, and S. Pratt, Phys. Rev. Lett. 85, 2689 (2000).

11. V. Vechernin, Symmetry 14, 21 (2022).

12. C. Alt, et al. (NA49 Collaboration), Phys. Rev. C 71, 034903 (2005).

13. M.M. Aggarwal, et al. (STAR Collaboration), Phys. Rev. C 82, 024905 (2010).

14. B.I. Abelev, et al. (STAR Collaboration), Phys. Lett. B 690, 239 (2010).

15. L. Adamczyk, et al. (STAR Collaboration), Phys. Rev. C 94, 024909 (2016).

16. B. Abelev, et al. (ALICE Collaboration), Phys. Lett. B 723, 267 (2013).

17. J. Adam, et al. (ALICE Collaboration), Eur. Phys. J. C 76, 86 (2016).

18. S. Acharya, et al. (ALICE Collaboration), Phys. Rev. C 100, 044903 (2019).

19. A. Tumasyan, et al. (CMS Collaboration), arXiv:2307.11185.

20. V. Abgaryan, et al. (MPD Collaboration), Eur. Phys. A 58, 140 (2022).

21. I. P. Lokhtin, L. V. Malinina, S. V. Petrushanko, et al., Comput. Phys. Commun. 180, 779 (2009).

22. I. P. Lokhtin, L. V. Malinina, S. V. Petrushanko, et al., Phys. At. Nucl. 73, 2139 (2010).

23. A. S. Chernyshov, G. Kh. Eyyubova, V.L. Korotkikh, et al., Chin.Phys. C 47, 084107 (2023).

24. D. Drijard et al. Nucl. Phys. B 166, 233 (1980).

25. J. Fu. J. Phys. G: Nucl. Part. Phys. 38, 065104 (2011).

26. 26. S. Pratt, C. Plumberg. Phys. Rev. C 104, 014906 (2021).

27. I. P. Lokhtin and A. M. Snigirev, Eur. Phys. J. C 45, 211 (2006).

28. T. Sjostrand, S. Mrenna, and P. Skands, JHEP 0605, 026 (2006).

29. T. Sjostrand, S. Mrenna, and P. Skands, Comput. Phys. Commun. 178, 852 (2008).

30. N. S. Amelin, R. Lednicky, T. A. Pocheptsov, et al., Phys. Rev. C 74, 064901 (2006).

31. N. S. Amelin, R. Lednicky, I. P. Lokhtin, et al., Phys. Rev. C 77, 014903 (2008).

32. G. Torrieri, S. Steinke, W. Broniowski, et al. Comput. Phys. Commun. 167, 229 (2005).

33. L. Adamczyk, et al. (STAR Collaboration), Phys. Rev. C 96, 044904 (2017).

34. A.V. Belyaev, L.V. Bravina, A.S. Chernyshov, et al. J. Phys. Conf. Ser. 1690, 012117 (2020).

35. O. Kodolova, M. Cheremnova, I. Lokhtin, et al. Phys. Part. Nucl. 52, 658 (2021).

36. M. Cheremnova, A. Chernyshov, Ye. Khyzhniak, et al. Symmetry 14, 1316 (2022).

37. S.A. Bass, M. Belkacem, M. Bleicher, et al. Prog. Part. Nucl. Phys. 41, 255 (1998).